

Modeling Solid-State Phase Transformations and Microstructure Evolution

L.Q. Chen, C. Wolverton, V. Vaithyanathan,
and Z.K. Liu

Introduction

The last decade or so has seen exciting developments in the field of modeling solid-state phase equilibria and phase transformations. In this article, we highlight three areas where such significant advancements have taken place, and demonstrate that linking these three approaches may yield an even more powerful tool for modeling solid-state phase transformations and microstructure evolution during the processing of multicomponent commercial materials: (1) first-principles atomistic calculations, (2) phase-field modeling of the temporal microstructure evolution, and (3) computational thermodynamics.

First-principles atomistic calculations, based on density-functional theory, do not rely on empirical input and hence are predictive in nature. These methods yield quantities related to the electronic structure and total energy of a given system, and may be used to accurately predict zero-temperature phase stabilities of alloys and compounds. By combining first-principles techniques with statistical mechanics methods (e.g., as discussed in the next section), one opens the possibility of exploring, without any fitting parameters, thermodynamics phenomena such as phase-transformation temperatures and phase diagrams,^{1,2} short-range order,^{3,4} and anti-phase and interphase boundary energetics.⁵ Furthermore, these approaches are amenable to any phases of a given alloy system, not only the equilibrium phases.

Hence, first-principles techniques can provide a method to obtain properties of metastable phases, which are often crucial to mechanical properties (e.g., strengthening precipitates) but can be difficult to isolate and study experimentally.

Phase-field modeling, based on fundamental principles of thermodynamics and kinetics, has recently been established as a powerful method for predicting the temporal microstructure evolution during solid-state phase transformations^{6,7} (for applications of phase-field modeling to solidification microstructures, see the recent review by Boettinger et al.⁸). In a phase-field model, the nature of a phase transformation as well as the microstructures that are produced is described by a set of continuous order-parameter fields. The temporal microstructure evolution is obtained by solving field kinetics equations that govern the time-dependence of the spatially inhomogeneous order-parameter fields. This model does not make any *a priori* assumptions about the transient morphologies and microstructures that may appear during a phase-transformation path. The phenomenological nature of the phase-field model allows one to model the microstructure evolution for a wide variety of diffusional and diffusionless phase transformations such as precipitation reactions,⁹ ferroelectric transformations,^{10,11} martensitic transformations,¹² phase transformations under an applied stress,^{12–15} and phase transformations in

the presence of structural defects (e.g., dislocations).¹⁶

The development of *computational thermodynamics* approaches (often referred to as calculated phase-diagram, or CALPHAD, techniques) has made possible the prediction of thermodynamics phase boundaries in multicomponent commercial alloys, often with 10 components or more.^{17,18} The CALPHAD approach can yield phase relationships and thermodynamics properties in experimentally uninvestigated regions of multicomponent systems from the extrapolation of their lower-order systems.^{19–21} This approach forms the foundation for the emerging concept of system materials design.^{22,23}

Monte Carlo Simulations of Alloy Morphologies Using First-Principles Energetics

Although highly accurate for predicting alloy properties, first-principles methods are currently limited to relatively small systems with a few hundred atoms. A simple estimate of the number of atoms in a typical microstructure (assuming an fcc lattice constant of $\sim 4 \text{ \AA}$) yields $1 \mu\text{m}^3 = 62,500,000,000$ atoms. Additionally, the problem of microstructural evolution of precipitate morphologies in a disordered solid-solution matrix requires a statistical sampling of the configuration space involved. In other words, one might need to evaluate the energetics of hundreds of billions of atoms, in trillions of configurations, in order to accurately account for the thermodynamics of this microstructural problem from an atomistic approach. Therefore, the *direct* application of first-principles atomistic techniques to problems of alloy microstructure such as those described in this article is clearly impossible with the computation power available for the foreseeable future. Even the somewhat simpler problem of calculating bulk solid-solution free energies or equilibrium precipitate shapes can require a simulation cell containing thousands of atoms or more, sampled over millions of configurations. Here, we describe a tool that has recently made possible the extension of first-principles energetics to thermodynamics properties of alloy systems with hundreds of thousands of atoms:^{24,25} the *mixed-space cluster expansion (CE)*.

In the mixed-space CE technique, energetics from first-principles calculations for a number of small unit cell (typically ~ 10 atoms or fewer) structures are mapped onto a generalized Ising-like model.^{1,26} In the CE approach, one selects a single, underlying parent lattice (in this case, fcc) and specifies the occupations of each of the N lattice sites by an A atom or a B atom.

For each configuration σ , one assigns the spin-occupation variables, $S_i = \pm 1$, to each of the N sites. Within the Ising-like description of the mixed-space CE, the positional degrees of freedom are integrated out, leaving energy as a function of spin variables $\{S_i\}$, which reproduces the energies of *atomically relaxed configurations*.²⁷ The expression used for the formation enthalpy (the zero-pressure energy with respect to the compositional average of the alloy constituents) of any configuration σ in the mixed-space CE is

$$\Delta H = \sum_{\mathbf{k}} J(\mathbf{k}) |S(\mathbf{k})|^2 + \sum_f D_f J_f \Pi_f + \sum_{\mathbf{k}} \Delta E_{\text{CS}} |S(\mathbf{k})|^2, \quad (1)$$

where the J variables are the interaction energies (“effective cluster interactions”), f is a symmetry-distinct figure comprising several lattice sites (pairs, triplets, etc.), D_f is the number of figures per lattice site, J_f is the Ising-like interaction for the figure f , and the “lattice-averaged product” Π_f is defined as a product of the variables S_i over all sites of the figure f , averaged over all symmetry-equivalent figures of lattice sites. $J(\mathbf{k})$ and $S(\mathbf{k})$ are the lattice Fourier transforms of the real-space pair interactions and spin-occupation variables J_{ij} and S_i , respectively, and CS is the coherency strain energy, defined as the strain energy of bulk A and B required to maintain coherency along an interface with orientation \mathbf{k} .

The CE expression for ΔH contains three summations: (1) pair interactions, conveniently summed using the reciprocal-space concentration-wave formalism; (2) non-pair multibody (e.g., three-body, four-body) interactions expressed in real space, and (3) the coherency strain energy. In practice, this quantity may be calculated from the energy change when bulk solids A and B are deformed from their equilibrium cubic lattice constants a_A and a_B to a common lattice constant a_{\perp} in the direction perpendicular to \mathbf{k} . Using first-principles energetics mapped onto the form of Equation 1, one can determine for a given alloy system the interactions $J(\mathbf{k})$ and J_f , as well as the coherency strain, from a detailed quantum mechanical approach. The CE approach thereby retains the accuracy of first-principles energetics, while the Ising-like form for the energy is simple enough to enable Monte Carlo simulations with thousands of atoms sampled millions of times.

An example of this first-principles CE approach is shown in Figure 1, which shows the calculated equilibrium shapes of Guinier–Preston (GP) zones in Al-Cu.²⁴ Using a first-principles-constructed CE for Al-Cu, Monte Carlo simulations are performed, beginning at high temperatures (where a solid-solution phase is stable) and slowly cooling through the coherent phase boundary to lower temperatures. Since the CE is only defined for coherent fcc-based configurations, the incoherent equilibrium structures do not appear, and the coherent

phase stability is “exposed.” In this manner, we can determine not only the equilibrium shapes of coherent precipitates below the phase boundary, but also the coherent phase boundary itself, as well as solid-solution properties at higher temperatures. In Al-Cu, we have found a size-dependent transition in the equilibrium shape, from Cu(001) monolayers at small precipitate sizes to a bilayer Cu/Al/Al/Al/Cu at larger precipitate sizes.²⁴ This transition, which explains many of the observations of GP1/GP2 zones in Al-Cu (see, e.g., a summary of the controversy in Reference 28), can be explained in terms of the balance between the thermodynamics driving force (favoring the bilayer structure) and the interfacial energy penalty around the rim of the plate (favoring the monolayer structure).

One should note that in the Al-Cu example shown here, the Monte Carlo simulations select the preferred morphologies and ordering out of the astronomical number of 2^N possible arrangements of Al and solute atoms, where N can be as large as 250,000. Thus, for a given alloy system, it is possible from these simulations to make an unbiased *prediction* of not only the equilibrium shapes of individual precipitates, but also the specific ordering internal to the particles.

We next turn to the larger-length-scale problem of microstructure evolution, which is currently beyond the capabilities of atomistic methods. The phase-field methodology, in which the atomic degrees of freedom

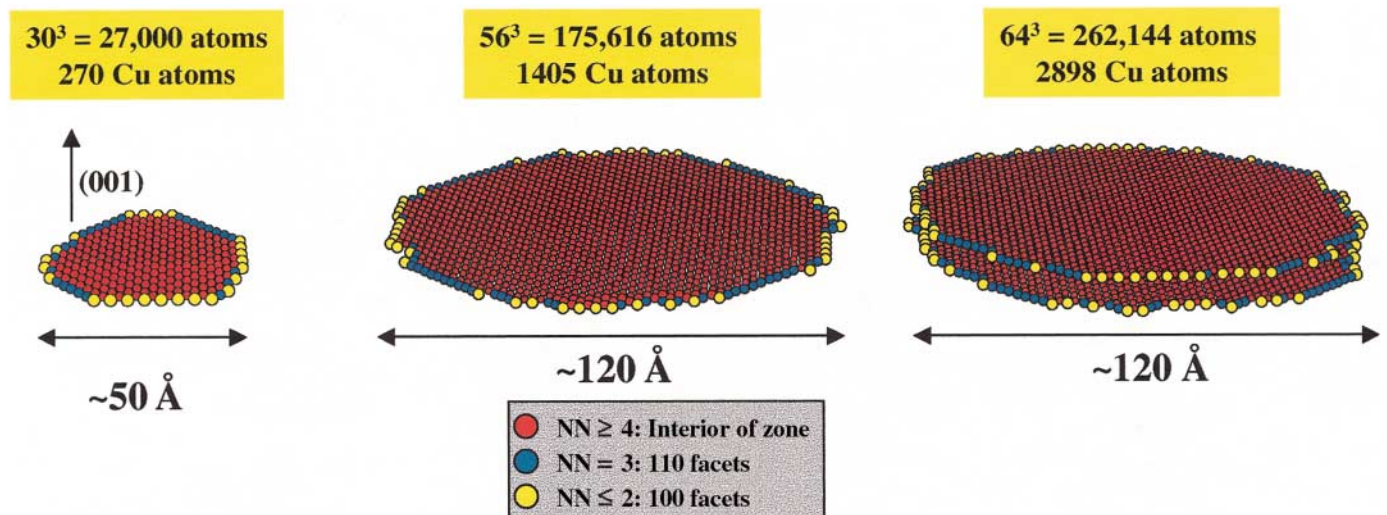


Figure 1. Equilibrium precipitate shapes of Guinier–Preston (GP) zones in Al-Cu, predicted from the first-principles mixed-space cluster expansion (CE) technique with Monte Carlo simulations. Results are shown for three simulations with progressively larger precipitate sizes with about 1% Cu. A change in the equilibrium shape is seen from a Cu(001) monolayer (GP1) at small sizes to a Cu/Al/Al/Al/Cu “sandwich” structure stacked along (001) (GP2) for larger precipitates. In each case, only the Cu atoms are shown, color-coded by the number of the 12 nearest neighbors (NN), which are also Cu.

are integrated out, provides a flexible framework for treating a wide variety of such microstructural problems.

Phase-Field Modeling of Coherent Phase Transformations

Phenomenologically, any phase transformation can be characterized by order parameters that distinguish the parent and product phases. For example, an order-disorder transformation can be described by a single or multicomponent long-range order parameter whose value is zero for the disordered phase and finite for the ordered phase. A simple idea to extend this order-parameter concept for microstructure evolution is to make the order-parameter fields spatially inhomogeneous and continuous; this idea embodies the diffuse-interface description of an inhomogeneous system.^{29,30} Information concerning the morphology and microstructure can be extracted from the spatial distribution of the order-parameter fields.

Within the diffuse-interface description, the thermodynamics of a phase transformation and the accompanying microstructure evolution are modeled by a free energy that is a function of all the order-parameter fields, or "phase fields." For a structural transformation, the total free energy can roughly be separated into the following three contributions:

$$F_{\text{tot}} = F_{\text{inc}} + F_{\text{int}} + F_{\text{elast}}, \quad (2)$$

where F_{inc} is the incoherent bulk free energy, F_{int} is the total interfacial free energy, and F_{elast} is the coherency elastic strain energy arising from the lattice accommodation along the coherent interfaces in a microstructure. For a microstructure described by a composition field c and a set of structural order parameters, $\eta_1, \eta_2, \dots, \eta_i$, the first two terms of Equation 2 are given by (see Reference 30 for the case of a composition field)

$$F_{\text{inc}} + F_{\text{int}} = \int_V \left[f(c, \eta_1, \eta_2, \dots, \eta_i) + a(\nabla c)^2 + \sum_i \beta_{jk}^i \frac{\partial \eta_i}{\partial r_j} \frac{\partial \eta_i}{\partial r_k} \right] dV, \quad (3)$$

where $f(c, \eta_1, \eta_2, \dots, \eta_i)$ is the local incoherent free-energy density as a function of composition and structural order parameters at a given temperature and pressure, and a and β_{jk}^i are gradient-energy coefficients.

An extensive discussion of the effect of elastic strain energy (F_{elast} in Equation 2) on microstructures produced from coherent structural phase transformations can

be found in the book by Khachaturyan.³¹ Various simulation methods for modeling coherent microstructures were recently reviewed by Fratzl.³² Most of the existing phase-field simulations of coherent phase transformations have assumed homogeneous elastic moduli.^{6,7} On the other hand, some simulations have included small elastic inhomogeneities by assuming that the elastic inhomogeneity is small and can therefore be modeled using first-order approximations.^{33–35} Recently, high-order methods have been proposed, and efficient numerical algorithms for directly solving the mechanical equilibrium equation have been developed.^{36–38} The calculated equilibrium displacements, and hence the elastic strain energy, are functions of composition and order-parameter fields.

With the total free energy of an inhomogeneous system written as a function of order-parameter fields, the temporal evolution of microstructures during a phase transformation can be obtained by solving the coupled Cahn–Hilliard nonlinear diffusion equation for a conserved field c and the time-dependent Ginzburg–Landau equation for a nonconserved field η_i .^{39,40}

$$\frac{\partial c}{\partial t} = \nabla \cdot \left[M \nabla \frac{\delta F_{\text{tot}}}{\delta c} \right] \quad (4)$$

and

$$\frac{\partial \eta_i}{\partial t} = -L_i \frac{\delta F_{\text{tot}}}{\delta \eta_i}, \quad (5)$$

where M is related to atom mobility and L_i is the relaxation constant associated with the order parameter η_i .

Numerical solutions to the set of kinetics equations (Equations 4–5) provide the temporal and spatial evolution of the order-parameter fields and thus describe the microstructure evolution. One of the main advantages of the field approach is that any arbitrary microstructure can be easily treated because there is no explicit tracking of the interface positions as in conventional sharp-interface modeling. In addition, various thermodynamics driving forces for microstructural evolution, including bulk chemical free energy, interfacial energy, and elastic strain energy, can be described with the same set of kinetics equations. Hence, different processes such as nucleation, growth, and coarsening can be described within a single, consistent physical and mathematical model.

One of the most studied examples using phase-field simulations is the precipitation process of a cubic intermetallic phase (γ') from a cubic disordered matrix (γ) in Ni-based superalloys.^{41–43} The precipitation

process is described by a compositional and a three-component order-parameter field. For this particular precipitation reaction, the order parameters are well defined physically and can be linked to microscopic quantities. This is different from solidification modeling, in which an auxiliary order-parameter field called a "phase field" is used as a way to distinguish a solid and a liquid, and as a mathematical convenience to avoid explicitly tracking the interface positions.⁸ The transformation strain for this precipitation reaction is dilatational and contains the information about a microstructure through its dependence on composition and order-parameter fields. A γ/γ' microstructure calculated from a three-dimensional phase-field simulation is shown in Figure 2.⁴⁴ The functional form of the bulk free energy is based on the symmetry considerations of the γ/γ' crystal structures, and the parameters entering the free energy are chosen to give the appropriate $\gamma + \gamma'$ two-phase equilibrium. The initial state is a homogeneous disordered Ni–Al alloy, γ . Upon annealing within the two-phase ($\gamma + \gamma'$) field, the γ' -ordered phase particles nucleate and grow in the disordered matrix. In a given microstructure, the particle shapes of relatively small particles are nearly spherical. As the particle sizes increase, their shapes gradually become cuboidal, and subsequently platelike, for relatively large particles. Since the interfacial energy is assumed to be isotropic in this particular simulation, the cuboidal and platelike shapes are entirely due to the anisotropic long-range elastic interactions. The particles tend to align along the crystallographically soft (minimum elastic modulus) directions ([001] in this case) during the precipitation process, and the degree of alignment increases as particle coarsening goes on. The strong particle–particle correlation is a manifestation of long-range elastic interactions among the precipitates. The predicted morphological and microstructure evolution agrees well with experimental observations in Ni-based superalloys⁴⁵ and is in general agreement with results obtained from other theoretical models.³² With the temporal microstructures, it is possible to analyze the size and size distributions of precipitates at any given moment, and hence the coarsening kinetics of precipitates can be determined.

Combined First-Principles/Phase-Field Calculations: Toward More Predictive Models of Microstructure

As the previous discussion illustrates, the continuum phase-field methodology is

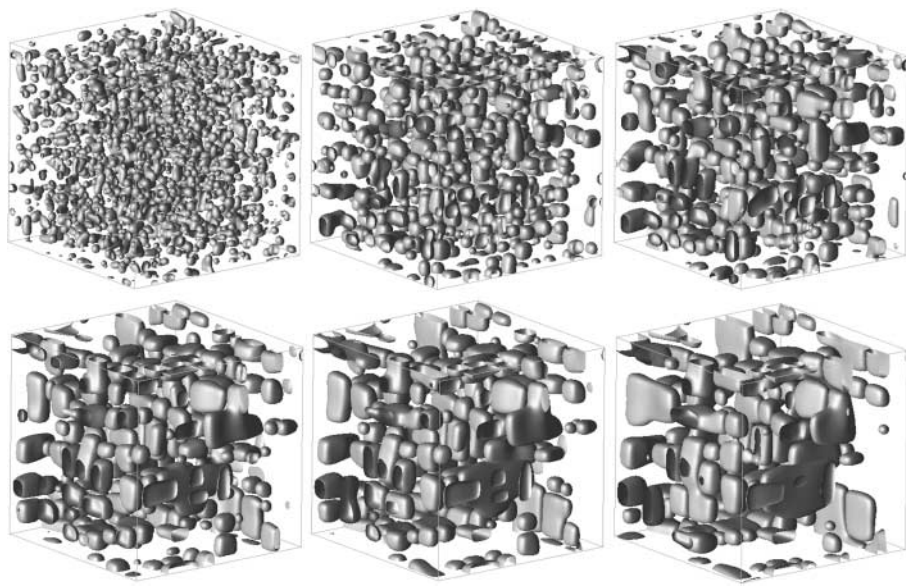


Figure 2. The temporal morphological evolution during precipitation of γ' -ordered particles from a γ matrix, predicted using a three-dimensional phase-field simulation.

able to predict complex alloy microstructures and their evolution during thermal aging. However, phase-field techniques often rely on empirical or difficult-to-measure physical quantities as input (e.g., Equation 2): (1) bulk free energies of solid-solution and precipitate phases, (2) precipitate/matrix interfacial free energies, and (3) precipitate/matrix lattice parameters and elastic properties. Often, the precipitate phases of interest are metastable, rather than equilibrium, phases, which can make experimental determination of these quantities problematic. What is required to make the phase-field calculations more predictive is a physically motivated method for accurately obtaining these input quantities. The combined first-principles/statistical mechanics approach just described can be used for such a purpose.

As we have explained, the *direct* application of first-principles atomistic techniques (limited to $\sim 10^2$ atoms) to problems of alloy microstructure (typically $\sim 10^{11}$ atoms), such as those described in this article, is clearly impossible. Even the mixed-space CE technique described for predicting coherent precipitate shapes is currently limited to 10^5 – 10^6 atoms, and hence is still not adequate for treating the micrometer length scale. However, from the combination of first-principles atomistic calculations, the mixed-space CE approach, and Monte Carlo simulations described here, it is possible to obtain each of the thermodynamics driving forces for microstructural evolution we have described: (1) The *bulk free energy* of the solid-

solution and precipitate phases may be obtained from Monte Carlo simulations of the type in Figure 2 coupled with thermodynamics integration techniques to obtain the free energy. (2) The precipitate/matrix *interfacial free energies* may be obtained from similar Monte Carlo simulations or from low-temperature expansion techniques. Alternatively, if only the $T = 0$ K values are needed, direct first-principles supercell calculations can also provide interfacial energies (i.e., without the need for a CE). (3) The *elastic strain energies* are of precisely the same form as the coherency strain energy used to generate the mixed-space CE. Hence, from a combination of first-principles atomistic calculations, a mixed-space CE approach, and Monte Carlo simulations, one can obtain all of the driving forces needed as input to a continuum phase-field model. The incorporation of these energetic properties, obtained from atomistics, into a continuum microstructural model represents a bridge between these two length scales and a real breakthrough in modeling capabilities: a “*first-principles*” model of alloy microstructural evolution.

We have recently applied this idea of linking first-principles and phase-field methodologies to the problem of θ' (Al₂Cu) precipitation in the Al-Cu system.⁴⁶ These θ' precipitates occur not only in binary Al-Cu alloys, but also are strengthening precipitates in a wide variety of industrial aluminum alloys. The phase-field model of Li and Chen¹⁴ was modified to include anisotropic interfacial energies, and the

input quantities for the model were generated from first-principles atomistics, as previously described. Thermodynamics integration of the CE for Al-Cu (used to generate GP zone shapes in Figure 1) yielded the solid-solution free energies. However, the problem of θ' precipitation is more complex here than in the earlier discussion of *coherent* precipitation, because θ' precipitates are not fully coherent with the Al matrix and θ' is not a superstructure of fcc (i.e., it is not formed by placing Al and Cu atoms on sites of a fully occupied fcc lattice). Therefore, the fcc CE used for the Al-Cu solid solution is not amenable to determining properties of θ' . For these properties, we appeal to direct first-principles calculations: the free energy of θ' is obtained from first-principles calculations of the $T = 0$ K energetics coupled with the calculated vibrational entropy of this phase, which has recently been found to be unexpectedly important in this system.⁴⁷ These bulk free energies of matrix and precipitate phases are then fit to the local free energy as a function of order-parameter fields in the phase-field model. $T = 0$ K interfacial energies are determined from supercell calculations, both for the coherent interface (along the face of the platelike θ' precipitates) and for the incoherent interface (around the rim of the plates). The anisotropy of these interfacial energies is large and is incorporated in the phase-field model. Coherency strain calculations of Al/Al₂Cu(θ') and the calculated lattice parameters of each phase determine the elastic strain driving force in this system. Thus, we have obtained all of the necessary thermodynamics input for the microstructural evolution of this system from an atomistic, predictive methodology. Figure 3 shows a preliminary example of phase-field simulation using thermodynamics driving forces obtained from first-principles calculations. The agreement between the calculated and observed microstructure of θ' in both binary and multicomponent alloys is excellent.⁴⁸ Extracting more quantitative microstructural information from these simulations, which are useful in understanding precipitation-hardening behavior, is under way.

The approaches discussed so far are for binary systems only. On the other hand, technologically important materials are typically multicomponent, with more than three components. In the next section, the current methodology of computational thermodynamics of multicomponent systems will be presented, followed by a road map showing how all three approaches described in this article may fall into a unified computational tool.

Computational Thermodynamics of Multicomponent Systems: A CALPHAD Approach

Computational thermodynamics is based on computer modeling of classical thermodynamics. In this approach, a large number of experimental data are used to extract parameters describing the alloy energetics, which are then used in calculations of thermodynamics properties, phase equilibria, phase diagrams, and phase transformations through the minimization of free energy and the calculation of thermodynamics driving forces. This approach has been developed primarily through the efforts of the CALPHAD community, and has reached the stage of being able to produce reliable phase diagrams and stability maps for complicated multicomponent commercial alloys.^{18–20,23}

Thermodynamics modeling begins with the evaluation of thermodynamics descriptions of unary and binary systems. By combining the evaluated constitutive binary systems and ternary experimental data, ternary interactions and the Gibbs energy of ternary phases are obtained. Thermodynamics databases thus developed cover the whole composition and temperature ranges, including experimentally uninvestigated regions. For example, in the Al-Fe-Si ternary system, in addition to the nine intermetallic compounds in the binary systems, there are seven ternary intermetallic compounds in the ternary system. Figure 4 presents the calculated liquidus projection for the Al-Fe-Si ternary system.⁴⁹ With the thermodynamics data developed, many types of quantities can be readily calculated, such as isopleth and isothermal sections, as shown in Reference 49. Based on the same procedure, thermodynamics descriptions of multicomponent systems have been developed and can be found on the Internet.^{50,51}

As just discussed, the CALPHAD approach is primarily based on available experimental data. However, in many cases, the amount of experimental data, especially thermochemical data, is not sufficient to provide a reliable thermodynamics description of the system. Furthermore, scattered and uncertain experimental data may be described equally well with different sets of model parameters. Such non-unique sets can yield disparate results for higher-order systems. These difficulties provide clear points of contact between the CALPHAD approach and the first-principles approaches. Whereas specific data may be difficult (or even impossible) to obtain experimentally, first-principles methods can often be employed to yield very accurate and physically clear energetic information.

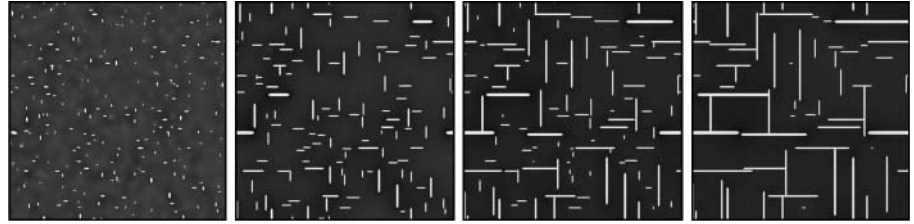


Figure 3. Temporal microstructure evolution during precipitation of tetragonal θ' particles (white) in a cubic matrix (black), obtained using a phase-field simulation with thermodynamics parameters from first-principle calculations.

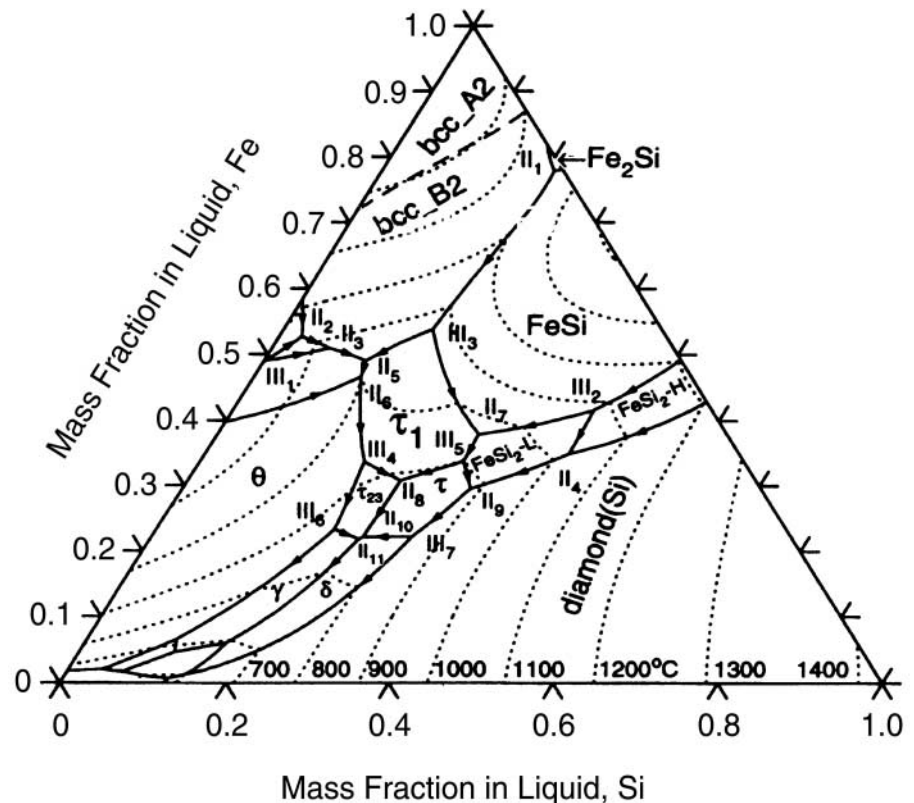


Figure 4. Liquidus projection of the Al-Fe-Si ternary system.

Summary and Outlook

In this article, we briefly outlined advances in three approaches for modeling the thermodynamics and microstructure evolution of phase transformations: first-principles calculations, phase-field simulation, and computational thermodynamics. The main advantages and disadvantages of each of these approaches have been discussed: Phase-field modeling is able to predict complex microstructure evolution during phase transformations, but it requires as input phenomenological thermodynamics and kinetics parameters. For binary systems, we have demonstrated that first-principles calculations can provide

physically meaningful thermodynamics input to phase-field simulations. However, it is unrealistic (for the foreseeable future) to assume that first-principles calculations can be used to determine all of the thermodynamics information for systems beyond ternary. On the other hand, semiempirical methods based on the CALPHAD approach are able to provide the bulk thermodynamics information of multicomponent systems, based on thermodynamics data in binary and ternary systems. Therefore, we would like to conclude this article by presenting a vision for linking these three approaches for multicomponent alloys (Figure 5): We suggest

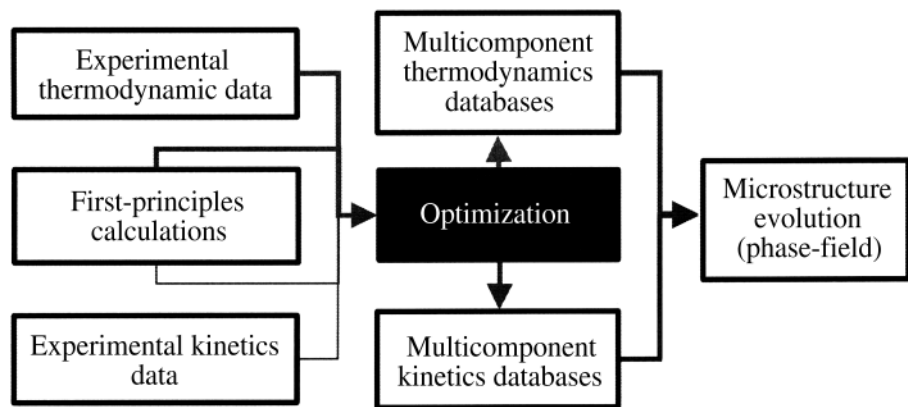


Figure 5. Schematic vision for linking first-principles calculations, computational thermodynamics and kinetics, and phase-field simulation of microstructure evolution.

that the development of a microstructure modeling tool for multicomponent systems of commercial interest requires the following three ingredients: (1) a multicomponent microstructure model, (2) reliable thermodynamics and kinetics databases for the multicomponent system, and (3) an interface linking (1) and (2).

The answer to the efficient development of multicomponent thermodynamics databases lies in a combination of approaches: the CALPHAD method, which is semi-empirical yet able to handle many components; first-principles calculations, which can provide critical thermodynamics data for binary systems, but are not able to deal with the complexities of the full multicomponent problem; and available experimental data. Analogous to the CALPHAD approach of thermodynamics database development, a combination of atomistic calculations, experimental data, and semiempirical treatment approaches will allow the construction of kinetics databases for multicomponent systems. Since phase-field models require input for thermodynamics and kinetics parameters, the next logical step is to build a multicomponent phase-field model with an interface to the thermodynamics and kinetics databases. Linking the three approaches described here with such an interface can yield a microstructure modeling tool for multicomponent systems that is even more powerful than any one of these approaches used alone. In principle, for a given alloy temperature and composition, a phase-field model, connected with experimentally constructed and first-principles-constructed thermodynamics and kinetics databases, could predict the temporal microstructure evolution in multicomponent systems of commercial interest.

References

1. A. Zunger, in *Statics and Dynamics of Alloy Phase Transformations*, NATO ASI Ser., edited by P.E.A. Turchi and A. Gonis (Plenum Press, New York, 1994) p. 361.
2. D. de Fontaine, *Solid State Phys.* **47** (1994) p. 33.
3. C. Wolverton, V. Ozolins, and A. Zunger, *J. Phys.: Condens. Matter* **12** (2000) p. 2749.
4. J.B. Staunton, D.D. Johnson, and F.J. Pinski, *Phys. Rev. B* **50** (1994) p. 1450.
5. M. Asta, in *Theory and Applications of the Cluster Variation and Path Probability Methods* (Plenum Press, New York, 1996) p. 237.
6. Y.Z. Wang, L.Q. Chen, and A.G. Khachatryan, in *Computer Simulation in Materials Science—Nano/Meso/Macroscopic Space and Time Scales*, NATO ASI Ser., edited by H.O. Kirchner, L. Kubin, and V. Pontikis (Ile d'Oleron, France, 1995).
7. L.Q. Chen and Y.Z. Wang, *JOM* **48** (1996) p. 13.
8. W.J. Boettinger, S.R. Coriell, A.L. Greer, A. Karma, W. Kurz, M. Rappaz, and R. Trivedi, *Acta Mater.* **48** (2000) p. 43.
9. Y.Z. Wang, L.Q. Chen, and A.G. Khachatryan, in *Solid-Solid Phase Transformations*, edited by W.C. Johnson, J.M. Howe, D.E. Laughlin, and W.A. Soffa (TMS, Warrendale, PA, 1994) p. 245.
10. H.L. Hu and L.Q. Chen, *J. Am. Ceram. Soc.* **81** (1998) p. 492.
11. S. Semenovskaya and A.G. Khachatryan, *J. Appl. Phys.* **83** (1998) p. 5125.
12. A. Artemev, Y. Wang, and A.G. Khachatryan, *Acta Mater.* **48** (2000) p. 2503.
13. D.Y. Li and L.Q. Chen, *Acta Mater.* **46** (1998) p. 639.
14. D.Y. Li and L.Q. Chen, *Acta Mater.* **46** (1998) p. 2573.
15. D. Orlikowski, C. Sagui, A.M. Somoza, and C. Roland, *Phys. Rev. B* **62** (2000) p. 3160.
16. S.Y. Hu and L.Q. Chen, *Acta Mater.* **49** (2001) p. 463.
17. L. Kaufman and H. Bernstein, *Computer Calculation of Phase Diagrams with Special Reference to Refractory Metals* (Academic Press, New York, 1970).
18. N. Saunders and A.P. Miodownik, *CALPHAD (Calculation of Phase Diagrams): A Comprehensive*

- Guide* (Pergamon Press, Oxford, 1998).
19. L. Kaufman, *J. Phase Equilib.* **14** (1993) p. 413.
 20. M. Hillert, *Scand. J. Metall.* **26** (1997) p. 215.
 21. C.J. Small and N. Saunders, *MRS Bull.* **24** (4) (1999) p. 22.
 22. G.B. Olson, *Science* **277** (1997) p. 1237.
 23. P.J. Spencer, *MRS Bull.* **24** (4) (1999) p. 18.
 24. C. Wolverton, *Philos. Mag. Lett.* **79** (1999) p. 683.
 25. C. Wolverton, *Model. Simul. Mater. Sci. Eng.* **8** (2000) p. 323.
 26. D.B. Laks, L.G. Ferreira, S. Froyen, and A. Zunger, *Phys. Rev. B* **46** (1992) p. 12587.
 27. C. Wolverton and A. Zunger, *Phys. Rev. Lett.* **75** (1995) p. 3162.
 28. V. Gerold, *Scripta Metall.* **22** (1988) p. 927.
 29. J.S. Rowlinson, *J. Stat. Phys.* **20** (1979) p. 197.
 30. J.W. Cahn and J.E. Hilliard, *J. Chem. Phys.* **28** (1958) p. 258.
 31. A.G. Khachatryan, *Theory of Structural Transformations in Solids* (John Wiley & Sons, New York, 1983).
 32. P. Fratzl, O. Penrose, and J.L. Lebowitz, *J. Stat. Phys.* **95** (1999) p. 1429.
 33. C. Sagui, D. Orlikowski, A.M. Somoza, and C. Roland, *Phys. Rev. E* **58** (1998) p. R4092.
 34. A. Onuki, *J. Phys. Soc. Jpn.* **58** (1989) p. 3065.
 35. H. Nishimori and A. Onuki, *Phys. Lett. A* **162** (1992) p. 323.
 36. P.H. Leo, J.S. Lowengrub, and H.J. Jou, *Acta Mater.* **46** (1998) p. 2113.
 37. S.Y. Hu and L.Q. Chen, *Acta Mater.*, submitted for publication, 2000.
 38. J.Z. Zhu, L.Q. Chen, J. Shen, and V. Tikare, *Phys. Rev. E*, submitted for publication, 2000.
 39. J.W. Cahn, *Acta Metall.* **9** (1961) p. 795.
 40. P.C. Hohenberg and B.I. Halperin, *Rev. Mod. Phys.* **49** (1977) p. 435.
 41. Y. Wang, D. Banerjee, C.C. Su, and A.G. Khachatryan, *Acta Mater.* **46** (1998) p. 2983.
 42. D.Y. Li and L.Q. Chen, *Acta Mater.* **47** (1999) p. 247.
 43. G. Rubin and A.G. Khachatryan, *Acta Mater.* **47** (1999) p. 1995.
 44. V. Vaithyanathan and L.Q. Chen, in *Nucleation and Growth Processes in Materials*, edited by A. Gonis, P.E.A. Turchi, and A.J. Ardell (Mater. Res. Soc. Symp. Proc. **580**, Warrendale, PA, 2000) p. 327.
 45. F. Li, S.V. Prikhodko, A.J. Ardell, and D. Kim, in *Proc. Int. Conf. on Solid-Solid Phase Transformations '99 (JIMIC-3)*, Vol. 12, edited by M. Koiwa, K. Otsuka, and T. Miyazaki (The Japan Institute of Metals, Sendai, 1999) p. 545.
 46. V. Vaithyanathan, C. Wolverton, and L.Q. Chen (unpublished).
 47. C. Wolverton and V. Ozolins (unpublished).
 48. T. Sato, T. Takahashi, N. Tanaka, and K. Mihama, *Japan J. Appl. Phys.* **21** (1982) p. L209; B. Skrotzki, G.J. Shiflet, and E.A. Starke Jr., *Metall. Mater. Trans. A* **27A** (1996) p. 3431.
 49. Z.K. Liu and Y.A. Chang, *Metall. Mater. Trans. A* **30A** (1999) p. 1081.
 50. C.W. Bale, Solution Databases, available from F*A*C*T Thermochemical Database Home Page, <http://www.crct.polymtl.ca/fact/fact.htm> (accessed February 2001).
 51. Thermodynamic Databases, available from Thermo-Calc Software, <http://www.thermo-calc.se/> (accessed February 2001). □